Check for updates

EurJIC
European Journal of Inorganic Chemistry

Research Article
doi.org/10.1002/ejic.202400243

Chemistry Europe
European Chemical Societies Publishing

www.eurjic.org

Thermally Stable Heteroleptic *Trans*-Bis(Chelate) Ruthenium(II) Complex Bearing 2,2′-Bipyridine and Acetylacetonato: Synthesis, Isomerization, and Crystal Structure

Mari Toyama,*[a, b] Daichi Fujimoto,[b] Yusuke Kawakami,[b] and Shiho Tanaka[b]

Thermally stable *trans*-bis(chelate)-type Ru(II) complexes are challenging to prepare owing to steric hindrance between the two chelate ligands. Herein, we investigated the isomerization of a heteroleptic *cis*-bis(chelate) complex to obtain its *trans* form. *cis*-[Ru(acac)(bpy)(dmso-*S*)$_2$](OTf)·0.5H$_2$O (**1**·(OTf)·0.5H$_2$O; acac$^-$ = acetylacetonato; bpy = 2,2′-bipyridine; dmso = dimethyl sulfoxide; OTf$^-$ = CF$_3$SO$_3^-$) was prepared by reacting *trans*(O,S)-[Ru(bpy)(dmso-*S*)$_2$(dmso-*O*)$_2$](OTf)$_2$ (**P0**) with Li(acac) in acetone at 298 K. In **1**·(OTf)·0.5H$_2$O, the two labile dmso-*O* ligands of **P0** were replaced by an acac$^-$ ligand. The dihedral angle between the chelate rings of bpy and acac$^-$ in **1**$^+$ was 76.7°, suggesting steric hindrance between ligands owing to the two bulky dmso-*S* ligands at the *cis* position. **1**·(OTf)·0.5H$_2$O was thermally stable in DMSO and acetone; however, in methanol and water, a dmso-*S* ligand was dissociated from **1**$^+$, and the complex isomerized to *trans*-[Ru(acac)(bpy)(dmso-*S*)(solvent)]$^+$. Refluxing of **1**·(OTf)·0.5H$_2$O in methanol for 18 h, evaporation to dryness under vacuum, and treatment with water yielded *trans*-[Ru(acac)(bpy)(dmso-*S*)(OH$_2$)](OTf) (**2**·(OTf)) with excellent purity. **2**·(OTf) was characterized by X-ray crystallography, elemental analysis, and ^{1}H NMR spectroscopy. As expected, steric hindrance was not observed between the *trans*-arranged bpy and acac$^-$, and the two chelates laid flat on the equatorial plane in **2**$^+$.

Introduction

Ru(II) complexes possessing one or more 2,2′-bipyridyne (bpy) ligands have been extensively studied owing to their unique photophysical and photochemical properties.[1–5] The stereochemistry of Ru(II) complexes with bpy holds great value in supramolecular chemistry, including stereo-controlled energy and electron transfer.[6–9] Although both *cis*- and *trans*-type building block complexes are necessary to prepare right-angled bent blocks and straight blocks, respectively, *trans*-type building block complexes are much less common than *cis*-type building block complexes. The *cis*-bis(2,2′-bipyridine)Ru(II) complex *cis*-[Ru(bpy)$_2$L$_2$]$^{2+}$ is a common *cis*-type building block complex. *cis*-Bis(bpy)Ru(II) complexes are well known to be isomerized by photoirradiation to the *trans*-isomer, whereas *trans*-bis(bpy)Ru(II) isomers are thermally unstable and isomerize to the corresponding *cis*-isomer owing to the steric hindrance between the H-6 protons of the bpy ligands within their equatorial plane.[10–16]

Coe et al. reported that *trans*-[RuCl(pdma)(N–N)(NO)](PF$_6$)$_2$ (pdma = 1,2-phenylenebis(dimethylarsine); N–N = 2,2′-bipyridine (bpy), 1,10-phenanthroline (phen), or 4,4′-dimethyl-2,2′-bipyridine) could be synthesized from the reaction of *fac*-[RuCl$_3$(pdma)(NO)] with excess bidentate N–N ligands by refluxing in methanol.[17] Mishra et al. synthesized *trans*-[Ru(PPh$_3$)$_2$(LH)$_2$](ClO$_4$)$_2$ (LH = 2-(2′-benzimidazolyl)pyridine) by reacting Ru(PPh$_3$)$_3$Cl$_2$ with 1,2-bis(2′-pyridylmethyleneimino)benzene in methanol under reflux, and characterized this complex using X-ray crystallography, elemental analysis, and ^{1}H NMR spectroscopy.[18] These *trans*-bis(chelate)Ru(II) complexes are thermally stable because of the absence of steric hindrance within the equatorial plane in the *trans*-Ru(bpy)$_2$ moiety. As uncommon bidentate ligands were used in these *trans*-type complexes, we aimed to construct *trans*-type complexes by combining popular bidentate ligands.

In a previous study, we reported the synthesis of a mono(bpy)Ru(II)-dmso complex, *trans*(O,S)-[Ru(bpy)(dmso-*S*)$_2$(dmso-*O*)$_2$](OTf)$_2$ (**P0**; dmso = dimethyl sulfoxide; OTf$^-$ = CF$_3$SO$_3^-$) bearing two labile dmso-*O* ligands in the axial and equatorial directions; this complex proved to be a good precursor for the synthesis of heteroleptic *cis*-bis(chelate)Ru(II) complexes, such as *cis*-[Ru(bpy)(phen)(dmso-*S*)$_2$](OTf)$_2$, which was selectively obtained in good yield (95 %) and excellent purity.[19] In this case, a slimmer chelate ligand, that is, the acetylacetonato ion (acac$^-$), was used instead of phen to obtain the thermally stable *trans*-Ru(acac)(bpy) complex.

[a] M. Toyama
Research Center for Safe Nuclear System Institute for Integrated Radiation and Nuclear Science, Kyoto University, 2-1010 Asashiro Nishi, Kumatori, Osaka 590-0494, Japan
E-mail: toyama.mari.3p@kyoto-u.ac.jp

[b] M. Toyama, D. Fujimoto, Y. Kawakami, S. Tanaka
Department of Chemistry of Functional Molecules, Faculty of Science and Engineering, Konan University, 8-9-1 Okamoto, Higashinada, Kobe 658-8501, Japan

Supporting information for this article is available on the WWW under https://doi.org/10.1002/ejic.202400243

Research Article
doi.org/10.1002/ejic.202400243

Chemistry Europe
European Chemical Societies Publishing

Acac$^-$ is a commercially available anionic chelate ligand. Many Ru(II)-acac complexes have been reported[20–28] because acac$^-$ is capable of tuning the redox potential of Ru complexes.[25] Moreover, acac$^-$ and other β-diketones are important compounds for medicinal chemists. Given their potential biological properties, synthetic accessibility, and metal-chelation ability, many complexes bearing a range of metals, including Ru(II), have been studied. For example, the anticancer properties of these complexes have been assessed.[21,26–28] Therefore, the synthesis and characterization of new Ru(II)-acac complexes is an important endeavor.

In this paper, the heteroleptic *cis*-bis(chelate) complex *cis*-[Ru(acac)(bpy)(dmso-*S*)$_2$](OTf)·0.5H$_2$O (**1**·(OTf)·0.5H$_2$O) was synthesized from the reaction of **P0** with Li(acac) in methanol at 298 K. Our ^{1}H NMR study showed that **1**·(OTf)·0.5H$_2$O was thermally stable in DMSO and acetone; however, in methanol and water, one dmso-*S* ligand was thermally dissociated from the molecule, and the complex isomerized to the *trans* complex *trans*-[Ru(acac)(bpy)(dmso-*S*)(solvent)]$^+$. When **1**·(OTf)·0.5H$_2$O was refluxed in methanol and the reaction mixture was treated with water, *trans*-[Ru(acac)(bpy)(dmso-*S*)(OH$_2$)](OTf) (**2**·(OTf)) was precipitated in excellent purity. The crystal structures of **1**·(OTf)·0.5H$_2$O and **2**·(OTf) were determined by single X-ray crystallography. The synthesis and characterization of a bis-heteroleptic *cis*-Ru(II)(acac)(bpy) complex and its thermal isomerization into a *trans*-Ru(II)(acac)(bpy) complex, as revealed in this study, could provide supramolecular chemistry with a unique building block that can to be isomerized in response to heat. Further, it may facilitate the design of new Ru(II)-acac complexes in medicinal chemistry.

Results and Discussion

Synthesis and Crystal Structure of 1·(OTf)·0.5H$_2$O

The synthetic route for **1**·(OTf)·0.5H$_2$O is shown in Scheme 1. In our previous report, the reaction of the precursor complex **P0**, in which the dmso-*O* ligands were more labile than the dmso-*S* ligands, with phen in acetone at 298 K selectively afforded the heteroleptic *cis*-bis(chelate) complex *cis*-[Ru(bpy)(phen)(dmso-*S*)$_2$](OTf)$_2$ in high yield (95%).[19] In the present study, Li(acac) was used instead of phen. The reaction of **P0** with Li(acac) in acetone at 298 K also afforded the heteroleptic *cis*-bis(chelate) complex *cis*-[Ru(acac)(bpy)(dmso-*S*)$_2$](OTf) in modest yield (78%). This result indicates that this method is suitable for the synthesis of heteroleptic *cis*-Ru(bpy)(chelate) complexes without any specific structural or charge requirements for a second chelating ligand. **1**·(OTf)·0.5H$_2$O was characterized by X-ray crystallography, elemental analysis, and ^{1}H NMR spectroscopy. X-ray-suitable crystals of **1**·(OTf)·0.5H$_2$O were obtained by the vapor diffusion of ethyl ether into an ethanol solution of **1**·(OTf)·0.5H$_2$O.

The crystallographic details for **1**·(OTf)·0.5H$_2$O are summarized in Table 1, and selected bond lengths and angles are provided in Table 2. The asymmetric unit contained half of a water molecule. Each of the hydrogen atoms of the water molecule in the crystals interacted with two O4 atoms of the dmso-S2 ligand in two **1**$^+$ complexes (Figure S1). An ORTEP drawing of the cation **1**$^+$ is shown in Figure 1.

The two Ru–N bond lengths (2.066(3) and 2.087(3) Å) were similar to those in **P0** (2.051(2) and 2.093(2) Å). The Ru1–N1 bond *trans* to the O atom of acac$^-$ was shorter than the Ru1–N2 bond *trans* to the S atom of the dmso-*S* ligand, due to the electronic effect of acac$^-$ at the *trans* position. The two Ru–O bonds (2.072(2) and 2.057(2) Å) in **1**$^+$ were comparable with those in *fac*(S)-[Ru(acac)Cl(dmso-*S*)$_3$] and *fac*(S)-[Ru(acac)(dmso-*S*)$_3$(dmso-*O*)](PF$_6$) (2.0640(13)–2.0751(13) Å) and [Ru(acac)(bpy)$_2$](PF$_6$)·CH$_2$Cl$_2$ (2.0591(11) and 2.0703(11) Å).[20,21]

The Ru1–S1 bond at the axial position (2.2386(10) Å) was shorter than the Ru1–S2 bond at the equatorial position (2.2812(8) Å), which was similar to the corresponding equatorial Ru–S bond in **P0** (2.2723(5) Å). The contraction of the Ru1–S1 bond may have been due to the electronic effect of acac$^-$ at the *trans* position. The torsion angle for O4–S2–Ru1–N1 was ~32.83°, and the O4 atom of the dmso-S2 ligand was forward to the H-6 proton of the pyridyl-N1 group of the bpy ligand. The distance between the O4 atom and H-6 of the pyridyl-N1 group was 2.293 Å, indicating the presence of an O···H–C hydrogen-bonding interaction. The angle of S2–Ru1–N1, at 99.67(7)°, was larger than ideal (90°) owing to the steric interaction between the rigid bpy and bulky dmso-S2 ligands within the equatorial plane. The two methyl groups of the axial dmso-S2 ligand were located above each of the two pyridyl rings of the bpy ligand. The shortest distance between two dmso ligands was 2.321 Å, which was between the proton of the methyl-C18 group of the

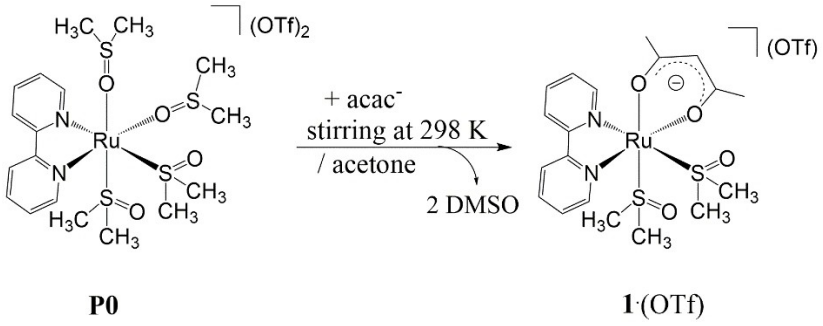

Scheme 1. Synthetic route for **1**·(OTf).

Research Article
doi.org/10.1002/ejic.202400243

Table 1. Crystallographic data for **1**·(OTf)·0.5H_2O and **2**·(OTf).

	1·(OTf)·0.5H_2O	**2**·(OTf)
Chemical Formula	$RuF_3S_3C_{20}N_2O_{7.5}H_{28}$	$RuF_3S_2C_{18}N_2O_7H_{23}$
Formula Weight	670.70	601.57
Temperature (K)	173	173
Crystal Dimensions (mm)	0.10×0.10×0.10	0.30×0.30×0.10
Color	yellow	orange
Crystal System	monoclinic	monoclinic
Space Group	*C2/c* (#15)	$P2_1/n$ (#14)
Lattice Parameters		
a (Å)	14.323(2)	7.23675(6)
b (Å)	12.739(2)	17.73420(16)
c (Å)	30.323(5)	18.16550(17)
α (°)	90	90
β (°)	100.7766(19)	100.1470(9)
γ (°)	90	90
V (Å^3)	5435.1(15)	2294.86(4)
Z	8	4
$D_{calcd.}$ (g/cm^3)	1.639	1.741
F_{000}	2728.00	1216.00
μ(Mo-/Cu–Kα, cm^{-1})	8.715	78.58
Independent Reflection	6236	4197
R1 [I > 2σ(I)]/No. of Reflections	0.0496/5711	0.0388/4042
wR2 (All Data)	0.1642/6236	0.1025/4197
GOF	1.357	1.036

Table 2. Selected bond lengths (Å), angles (deg), and dihedral angles (deg) for **1**·(OTf)·0.5H_2O and **2**·(OTf).

	1·(OTf)·0.5H_2O	**2**·(OTf)
Ru1–N1	2.066(3)	2.040(3)
Ru1–N2	2.087(3)	2.039(3)
Ru1–S1	2.2386(10)	2.1743(7)
Ru1–S2	2.2812(8)	—
Ru1–O1	2.072(2)	2.046(2)
Ru1–O2	2.057(2)	2.060(2)
Ru1–O4	—	2.141(2)
N1–Ru1–N2	78.73(10)	79.48(10)
O1–Ru1–O2	91.44(10)	91.99(9)
N1–Ru1–O2	83.38(10)	93.89(10)
N2–Ru1–O1	92.49(10)	94.04(9)
S1–Ru1–S2	91.78(4)	—
N1–Ru1–S2	99.67(7)	—
S2–Ru1–O1	91.08(7)	—
S1–Ru1–O2/O4	176.60(7)	177.91(8)

equatorial dmso-S2 ligand and the O3 atom of the axial dmso-S1 ligand. This proximity implied a C–H···O hydrogen-bonding interaction between two dmso-*S* ligands. Such conformations of two dmso-*S* ligands at the *cis* position in a Ru(II) complex have been observed in crystals of *cis*(Cl),*cis*(S)-[$RuCl_2$(bpy)(dmso-*S*)$_2$] and *trans*(S,N_{MeCN})-[RuCl(bpy)(dmso-*S*)$_2$(MeCN)](PF_6)·MeCN.[29,30]

The dihedral angle between the two five- and six-membered chelate rings of bpy and acac$^-$ was 76.7°, which was significantly smaller than the ideal angle (90°). In [Ru(acac)(bpy)$_2$](PF_6)·CH_2Cl_2, which does not contain bulky dmso-*S* ligands, the dihedral angles between the acac$^-$ and bpy chelate rings (81.6° and 81.9°) were closer to 90° than that of **1**$^+$.[21] This finding suggests that the larger dihedral angle between acac$^-$ and bpy in **1**$^+$ is caused by the methyl-C19 group of the equatorial dmso-S2 ligand pushing the acac$^-$ ligand. The conformation of the equatorial dmso-*S* ligand was restricted by the axial dmso-*S* and bpy ligands. Therefore, steric crowding occurs among the ligands in **1**$^+$, resulting in a slight tilt of acac$^-$ toward the bpy ligand.

Chemical Behavior of 1·(OTf)·0.5H_2O in Solution

The ^{1}H NMR spectrum of **1**·(OTf)·0.5H_2O in DMSO-d_6 is shown in Figure 2. Eight signals with intensities of 1H for the bpy ligand were observed at the aromatic region, and a singlet at 5.51 ppm for CH and two singlets for the two methyl groups of the acac$^-$ ligand appeared at the aliphatic region. These results indicate that the two pyridyl groups in bpy and two methyl groups in acac$^-$ were in different environments owing to the

Research Article
doi.org/10.1002/ejic.202400243

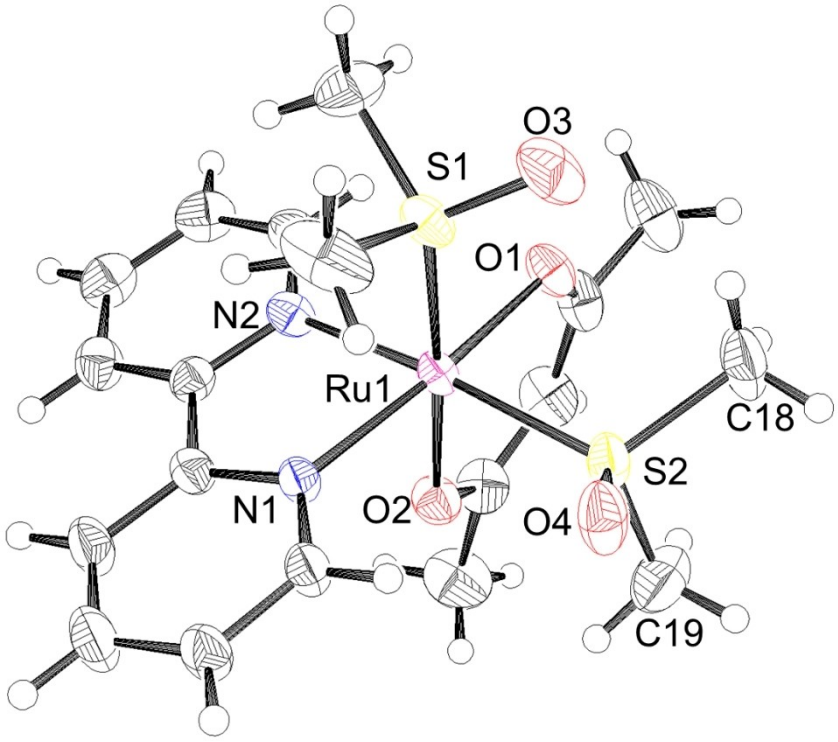

Figure 1. ORTEP drawing of the cation of **1**·(OTf)·0.5H_2O with 50% probability ellipsoids. A OTf^- anion and water molecule were omitted for clarity.

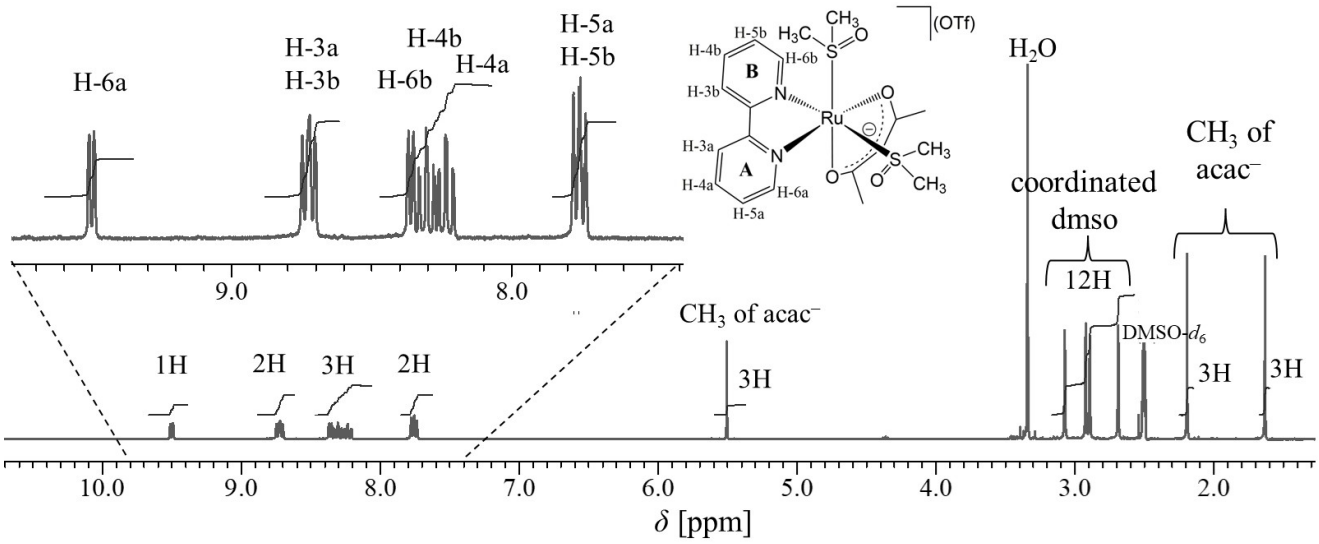

Figure 2. ^{1}H NMR spectrum of **1**·(OTf)·0.5H_2O in DMSO-d_6 (300 MHz at 293 K).

cis-Ru(acac)(bpy) geometry. Four signals with intensities of 3H for the four methyl groups of the two dmso-*S* ligands were also observed. This is reasonable because two dmso-*S* ligands in $\mathbf{1}^+$ existed in different environments, and the molecule is chiral. Thus, the methyl groups on each dmso-*S* ligand are diastereotopic with different chemical shifts. This spectrum corresponds to the crystal structure of **1**·(OTf)·0.5H_2O.

Although the chemical shifts of the two H-6 signals were relatively far, at 9.49 and 8.36 ppm, those of the corresponding protons for the two pyridyl groups in the bpy ligand were close. This finding indicates that the O4···H-6 of pyridyl-N1 hydrogen-bonding interaction, which was observed in the crystals, is maintained in DMSO solution. Thus, the pyridyl-N1 group was assigned to ring A. This attribution corresponds to the ^{1}H NMR spectral attribution of $[Ru(bpz)(terpy)(L)]^+$, where bpz = 2,2′-bipyrazine, terpy = 2,2′,2″-terpyridine, and X = Cl, H_2O, or CH_3CN)[31].

When **1**·(OTf)·0.5H_2O was heated in DMSO-d_6 at 363 K for 3 h, the four methyl signals in its NMR spectrum decreased and a signal assigned to free DMSO appeared, indicating that the

Research Article
doi.org/10.1002/ejic.202400243

two dmso-*S* ligands in **1**$^+$ were exchanged with DMSO-d_6 solvent molecules (Figure S2). Four new weak signals appeared in the aromatic region of the spectrum, which suggests that the two pyridyl groups of bpy were in the same environment; thus, the new complex must have the *trans*-Ru(acac)(bpy) conformation (Figure S3). The intensity of the four new signals in the NMR spectrum of **1**·(OTf)·0.5H_2O did not change after another 1 h of heating, and the *cis*-isomer/*trans*-isomer ratio was 95/5. Therefore, the *cis*-Ru(acac)(bpy) geometry is significantly more thermally stable than the *trans*-Ru(acac)(bpy) geometry in DMSO. **1**$^+$ was also thermally stable in acetone. When **1**·(OTf)·0.5H_2O was heated at 313 K for 4 h in acetone-d_6 solution, its NMR spectrum was identical to that before heating (Figure S4).

In methanol and water, a dmso-*S* ligand was thermally dissociated from **1**$^+$, and the complex isomerized from the *cis*- to the *trans*-Ru(acac)(bpy) geometry. The ^{1}H NMR spectra of **1**·(OTf)·0.5H_2O in CD_3OD are shown in Figure 3. After heating at 323 K for 3 h, the signals for **1**$^+$ decreased and four new signals for the coordinated bpy clearly appeared in the aromatic region; a signal for free DMSO was also observed at 2.65 ppm. After heating for another 12 h, the signals for **1**$^+$ nearly completely disappeared from the spectrum, and only the four signals of the new complex, which had the *trans*-Ru(acac)(bpy) geometry, were observed. In the aliphatic region, the signal of the maintained coordinated dmso ligand was observed at 2.79 ppm, and the signal for another dmso ligand that was released from a Ru^{2+} ion to become a free DMSO molecule was noted at 2.65 ppm. The equivalent signals of the two methyl groups of acac$^-$ were also observed at 2.19 ppm. The structure of the new thermally stable complex would be *trans*-[Ru(acac)(bpy)(dmso)(CD_3OD)]$^+$. *cis*-[Ru(acac)(bpy)(dmso-*S*)(CD_3OD)]$^+$ was not observed during isomerization on the ^{1}H NMR timescale, indicating that isomerization occurred simultaneously with the release of the dmso ligand from **1**$^+$ and was likely caused by it. Based on the assumption that isomerization is a pseudo-first-order reaction, the reaction rate constant k at 323 K was determined from the integral ratio of the CH signals of the acac$^-$ ligand of **1**$^+$ and *trans*-[Ru(acac)(bpy)(dmso-*S*)(CD_3OD)]$^+$ in the ^{1}H NMR spectra using the initial rates method. The plot of the natural function of the decrease degree of **1**$^+$ versus heating time (sec) is linear (Figure S5), yielding a *k* of $5.7(2)\times10^{-5}$ s^{-1} ($t_{1/2}=3.4(1)$ h). The results provide evidence that the isomerization reaction can be regarded as a pseudo-first-order reaction, where the isomerization of *cis*- to *trans*-geometry form occurs simultaneously with the dissociation of one dmso from **1**$^+$.

The leaving dmso-*S* ligand would be the equatorial one, based on the fact that the Ru1—S2 bond (between Ru^{2+} and equatorial dmso-*S*) was longer than the Ru1—S1 bond (between Ru^{2+} and axial dmso-*S*). In the crystal structure, the axial and equatorial dmso-*S* ligands were interlocked like gears and connected by CH···O hydrogen-bonding interactions. Thus, they acted similar to a bidentate ligand in **1**$^+$, thereby locking the *cis*-Ru(acac)(bpy) geometry. However, when the CD_3OD solvent molecule coordinated to Ru^{2+} upon the dissociation of the equatorial dmso-*S* ligand, it did not interact with the axial dmso-*S* ligand. This may have unlocked the *cis*-Ru(acac)(bpy) geometry, resulting in the migration of acac$^-$ to the *trans* position of bpy. In DMSO, isomerization did not occur, suggesting that the exchange reaction between the dmso-*S* ligands and DMSO-d_6 was faster than isomerization. Additionally, isomerization did not occur because a dmso-*S* ligand did not dissociate in acetone. A similar thermal isomerization reaction was observed in D_2O, forming *trans*-[Ru-

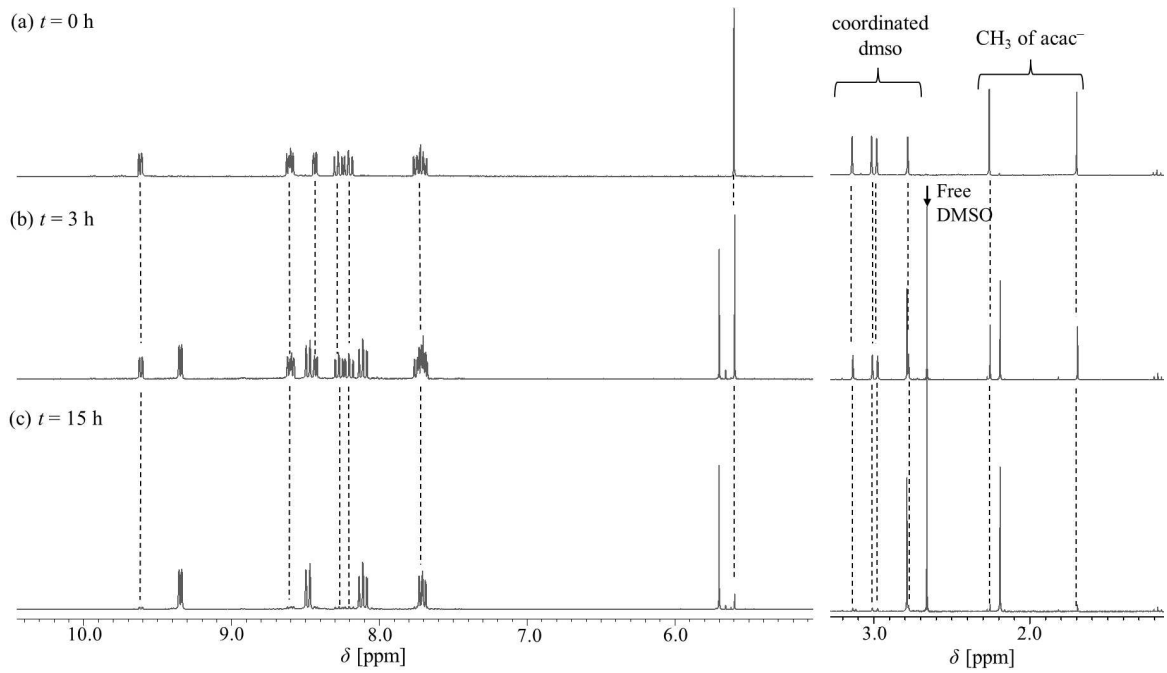

Figure 3. ^{1}H NMR spectra of **1**·(OTf)·0.5H_2O in CD_3OD (300 MHz at 293 K) after heating for *t* h at 323 K.

Research Article
doi.org/10.1002/ejic.202400243

(acac)(bpy)(dmso-*S*)(D_2O)]$^+$ and a free DMSO molecule (Figure S6).

Synthesis and Characterization of 2·(OTf)

The synthetic route for **2**·(OTf) is shown in Scheme 2. Refluxing of a methanol solution of **1**·(OTf)·0.5H_2O afforded *trans*-[Ru(acac)(bpy)(dmso-*S*)(MeOH)]$^+$. Following evaporation of the reaction solution, *trans*-[Ru(acac)(bpy)(dmso-*S*)(MeOH)](OTf) and free DMSO molecules remained in the residue. When the residue was treated with ethyl ether to isolate *trans*-[Ru(acac)(bpy)(dmso-*S*)(MeOH)](OTf), a mixture of *trans*-[Ru(acac)(bpy)(dmso)$_2$](OTf), **1**·(OTf)·0.5H_2O, and a small amount of unknown material was obtained. Hence, we abandoned the isolation of *trans*-[Ru(acac)(bpy)(dmso-*S*)(MeOH)](OTf). When a small amount of water was added to the residue, the orange complex *trans*-[Ru(acac)(bpy)(dmso-*S*)(OH_2)](OTf) (**2**·(OTf)) was spontaneously precipitated, and the free DMSO molecules remained in the water. The structure of **2**·(OTf) was determined by ^{1}H NMR spectroscopy, elemental analysis, and single-crystal X-ray analysis.

The aromatic region of the ^{1}H NMR spectrum of **2**·(OTf) in D_2O is shown in Figure S7. The ^{1}H NMR spectrum revealed that the two pyridyl groups of the bpy ligand and the two methyl groups of the acac$^-$ ligand in **2**$^+$ were in the same environment; thus, the complex had the *trans*-Ru(acac)(bpy) conformation. The spectrum of this complex agreed with that of **1**·(OTf)·0.5H_2O heated in D_2O (Figure S6). In the aliphatic region, the signal of the dmso-*S* ligand in **2**$^+$ was observed at 2.16 ppm, and its intensity was 6H. This finding showed that the two methyl groups were equivalent, which corresponds with the crystal structure.

Orange crystals suitable for X-ray crystallography were obtained by concentrating an aqueous solution of **2**·(OTf) at 298 K. In the crystals, a H atom of the aqua-O4 ligand in **2**$^+$ exhibited a hydrogen-bonding interaction with the O3* atom of the dmso-S1 ligand in an adjacent **2**$^+$. Another H atom of the aqua-O4 ligand in **2**$^+$ also exhibited a hydrogen-bonding interaction with the O5 atom in the OTf$^-$ anion. Therefore, a 1-D hydrogen-bonding network existed along the *a* axis (Figure S8). The bpy site of the 1-D hydrogen-bonding chain overlapped the bpy site of the adjacent 1-D hydrogen-bonding chain. The distance between each bpy ligand was approximately 3.3 Å, suggesting a π–π stacking interaction.

An ORTEP drawing of the cation **2**$^+$·is shown in Figure 4, and selected bond lengths and angles are provided in Table 2. The dihedral angle between the two chelate rings of bpy and acac$^-$ was 10.0°, indicating that these two ligands were almost within the same plane. Two H-6 protons of the bpy ligands in **2**$^+$ exhibited contact with the coordinated O atoms of acac$^-$ (2.562 and 2.576 Å), thus suggesting CH···O interactions between these ligands.

The two Ru–N bond lengths (2.039(3) and 2.040(3) Å) were identical, and these were shorter than those in **1**$^+$ (2.066(3) and 2.087(3) Å) because **2**$^+$ has less steric interactions than **1**$^+$. Moreover, these bond lengths were similar to those of the Ru–N(bpy) *trans* to the O atoms of acac$^-$ in [Ru(acac)(bpy)$_2$](PF_6)·CH_2Cl_2 (2.0240(13) and 2.0316(13) Å).[21] The Ru1–S1 bond length (2.1743(7) Å) was clearly shorter than that in **1**$^+$. The Ru1–O4 bond length (2.141(2) Å) was similar to the corresponding Ru–O(OH_2) bond lengths in *trans*(O,S)-[RuCl(bpy)(dmso-*S*)$_2$(OH_2)](PF_6)·H_2O (2.137(2) Å), *cis*-[Ru(bpy)$_2$(OH_2)$_2$](PF_6)$_2$ (2.129(4)–2.152(5) Å), and *trans*-[Ru(bpy)$_2$(OH_2)$_2$](OTf)$_2$ (2.1053(16) Å).[11,12,30]

2·(OTf) was soluble in water, alcohols, and some organic solvents, and the aqua ligand in **2**$^+$ was generally labile. The ^{1}H NMR spectrum of **2**·(OTf) in CD_3CN revealed four signals at the aromatic region; the signal for the aqua ligand was not observed. In CD_3CN, the aqua ligand in **2**·(OTf) is probably quickly exchanged to form *trans*-[Ru(acac)(bpy)(dmso-*S*)(CD_3CN)](OTf) (Figure S9). After photoirradiation of the NMR sample for 15 min by a 300 W Xe-lamp, its ^{1}H NMR spectrum exhibited four small signals in the aromatic region as well as the peaks of free DMSO at 2.50 ppm. This result suggests that the coordinated dmso-*S* ligand is released to produce *trans*-[Ru(acac)(bpy)(CD_3CN)$_2$]$^+$. Our findings suggest that **2**·(OTf) has unique potential as a *trans*-building block complex. Because the two monodentate ligands in **2**$^+$ differ in their substitution capacity, incorporating two different bridging ligands in axial sites may be possible.

Conclusions

The heteroleptic *cis*-bis(chelate)Ru(II) complex *cis*-[Ru(acac)(bpy)(dmso-*S*)$_2$](OTf)·0.5H_2O (**1**·(OTf)·0.5H_2O) was synthesized from the reaction of *trans*(O,S)-[Ru(bpy)(dmso-*S*)$_2$(dmso-*O*)$_2$](OTf)$_2$ (**P0**) with Li(acac) in acetone at 298 K. X-ray crystallography revealed that **1**·(OTf)·0.5H_2O had an acac$^-$ ligand and a

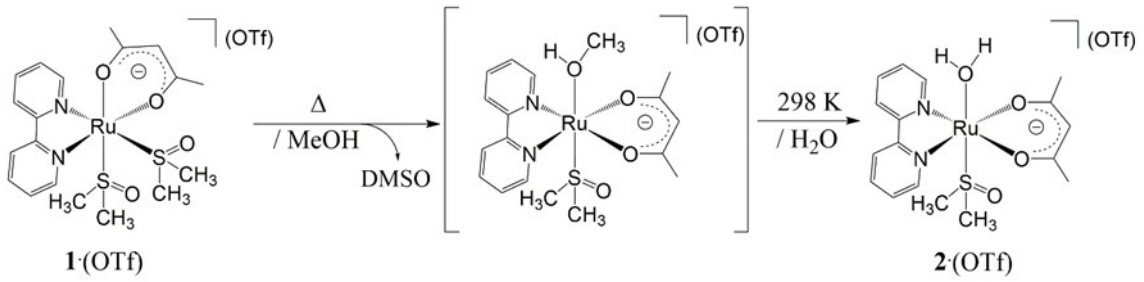

Scheme 2. Synthetic route for **2**·(OTf).

Research Article
doi.org/10.1002/ejic.202400243

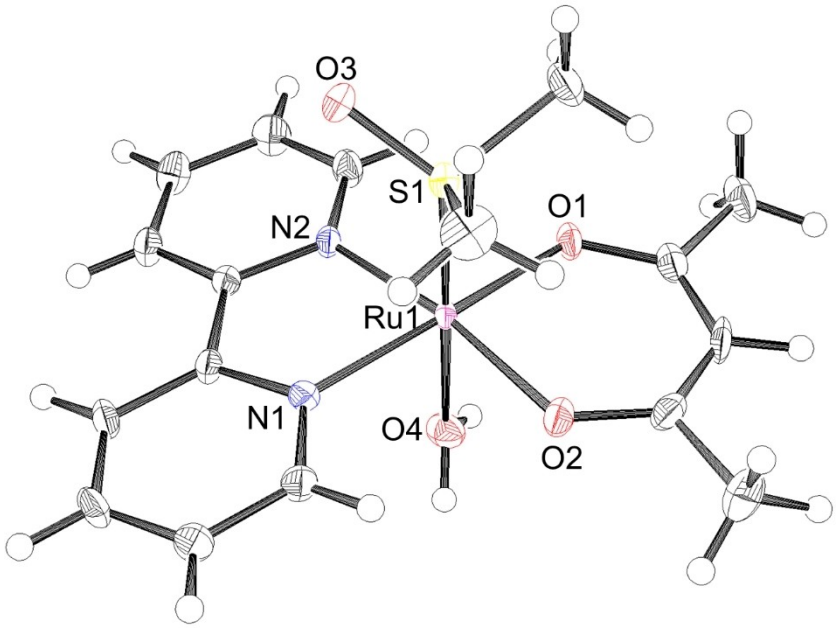

Figure 4. ORTEP drawing of the cation of **2**·(OTf) with 50% probability ellipsoids. A OTf⁻ anion was omitted for clarity.

bpy ligand at the *cis* position; thus, the two dmso-*O* ligands in **P0** were substituted by acac⁻. The dihedral angle between the chelate rings of the acac⁻ and bpy ligands in $\mathbf{1}^+$ was 76.7°, which suggests the presence of steric hindrance between ligands owing to the two bulky dmso-*S* ligands at the *cis* position. The bulky equatorial dmso-*S* ligand, which was restricted by CH···O hydrogen-bonding interactions with bpy, and the axial dmso-*S* ligands slightly pushed the acac⁻ ligand toward bpy. Thus, the equatorial dmso-*S* ligand locked the *cis*-Ru(acac)(bpy) geometry.

^{1}H NMR spectroscopy showed that $\mathbf{1}^+$ was thermally stable in DMSO-d_6 and acetone-d_6; however, in CD_3OD and D_2O, a dmso-*S* ligand was thermally dissociated from the molecule, and the complex isomerized to *trans*-[Ru(acac)(bpy)(dmso-*S*)(solvent)]$^+$. **1**·(OTf)·0.5H_2O was refluxed in methanol and then treated with water to precipitate *trans*-[Ru(acac)(bpy)(dmso-*S*)(OH_2)](OTf) (**2**·(OTf)), which was characterized using ^{1}H NMR spectroscopy, elemental analysis, and X-ray crystallography. In the crystal structure of $\mathbf{2}^+$, the dihedral angle between the chelate rings of the acac⁻ and bpy ligands was 10.0°, indicating that these two ligands are nearly coplanar. Naturally, bpy and acac⁻ are not sterically influenced by two monodentate ligands at the axial position. **2**·(OTf) was highly soluble in water, alcohol, and organic solutions, and the aqua ligand in $\mathbf{2}^+$ can easily be substituted. Therefore, **2**·(OTf) is a useful thermally stable *trans*-type building block that contains bpy. Moreover, because $\mathbf{2}^+$ has two different monodentate ligands with different substitution abilities at the axial position, the complex may be incorporated with two different bridging ligands at these sites. In future research, we will synthesize dinuclear complexes that can change structure in response to heat in methanol and water using $\mathbf{1}^+$ with a *cis*-Ru(II)(acac)(bpy) unit and complex linear coordinating polymers, as well as $\mathbf{2}^+$ with a *trans*-Ru(II)(acac)(bpy) unit containing different binding ligands. We will also investigate their structures and characteristics.

Experimental Section

General Experimental Details

The starting material *cis*(S),*cis*(O)-[Ru(bpy)(dmso-*S*)$_2$(dmso-*O*)$_2$](OTf)$_2$ (**P0**) was prepared according to the literature,[19] and **1**·(OTf)·0.5H_2O was prepared using the synthetic method for *cis*-[Ru(bpy)(phen)(dmso-*S*)$_2$](OTf)$_2$.[19] All reactions were carried out under an Ar atmosphere.

^{1}H NMR spectra were recorded in DMSO-d_6, acetone-d_6, CD_3OD, and D_2O at 293 K using a Varian Mercury 300 spectrometer (300 MHz). TMS (for DMSO-d_6, acetone-d_6, and CD_3OD) and DMSO (for D_2O, 2.71 ppm in D_2O) were used as internal standards.[32] The aromatic signals were assigned on the basis of their coupling constants and ^{1}H-^{1}H COSY experiments (Figure S10).[33] The ^{1}H NMR spectroscopic data for **1**·(OTf)·0.5H_2O in acetone-d_6 and D_2O are shown in Figures S11 and S12, respectively. Absorption spectra were recorded at 298 K using a HITACHI U-3310 spectrometer. The absorption spectra and associated data of **1**·(OTf)·0.5H_2O in DMSO and **2**·(OTf) in water are shown in Figures S13 and S14, respectively.

Synthesis of *cis*-[Ru(acac)(bpy)(dmso-*S*)$_2$](OTf)·0.5H_2O (**1**·(OTf)·0.5H_2O)

A mixture of **P0** (1.06 g, 1.2 mmol) and Li(acac) (0.15 g, 1.4 mmol) in acetone (100 mL) was stirred for 10 h at 298 K. The yellow solution gradually turned dark brown. The resulting dark-brown solution was evaporated to dryness under vacuum. The residue was dissolved in ethanol (3 mL), and ethyl ether (50 mL) was added to precipitate the brown complex *cis*-[Ru(acac)(bpy)(dmso-*S*)$_2$](OTf)·0.5H_2O (**1**·(OTf)·0.5H_2O). The brown precipitate was washed by decantation with a small amount of ethyl ether. The precipitate

was collected by filtration, washed with a small amount of ethyl ether, and dried in vacuo (0.63 g, 78%). Yellow crystals suitable for X-ray crystallography were obtained by the vapor diffusion of ethyl ether into an ethanol solution of **1**·(OTf)·0.5H_2O. $C_{20}H_{27}F_3N_2O_7RuS_3$ (670.70): calcd. C 36.30, N 4.23, H 4.11; found C 35.81, N 4.18, H 4.21. ^{1}H NMR (300 MHz, DMSO-d_6): δ 9.50 (d, ^3J=5.6 Hz, H-6a), 8.72 (m, 2H, H-3a and H-3b), 8.36 (d, ^3J=5.6 Hz, H-6b), 8.30 (t, ^3J=7.9 Hz, H-4b), 8.23 (t, ^3J=7.9 Hz, H-4a), 7.76 (m, 2H, H-5a and H-5b), 5.51 (s, 1H, CH of acac$^-$), 3.07 (s, 3H, CH_3 of dmso), 2.92 (s, 3H, CH_3 of dmso), 2.89 (s, 3H, CH_3 of dmso), 2.69 (s, 3H, CH_3 of dmso), 2.19 (s, 3H, CH_3 of acac$^-$), 1.63 (s, 3H, CH_3 of acac$^-$) ppm. ^{1}H NMR (300 MHz, CD_3OD): δ 9.62 (d, ^3J=5.7 Hz, H-6a), 8.61 (d, ^3J=8.2 Hz, H-3b), 8.60 (d, ^3J=8.2 Hz, H-3a), 8.44 (d, ^3J=5.6 Hz, H-6b), 8.28 (dd, ^3J=7.6 and 8.2 Hz, H-4b), 8.21 (dd, ^3J=7.5 and 8.1 Hz, H-4a), 7.75 (dd, ^3J=5.6 and 7.6 Hz, H-5b), 7.70 (dd, ^3J=5.7 and 7.5 Hz, H-5a), 5.60 (s, 1H, CH of acac$^-$), 3.14 (s, 3H, CH_3 of dmso), 3.02 (s, 3H, CH_3 of dmso), 2.99 (s, 3H, CH_3 of dmso), 2.78 (s, 3H, CH_3 of dmso), 2.28 (s, 3H, CH_3 of acac$^-$), 1.70 (s, 3H, CH_3 of acac$^-$) ppm. Absorption spectroscopic data in DMSO (nm, M^{-1} cm^{-1}): 340 (4.4×10^3) and 400 (2.5×10^3).

Synthesis of *trans*-[Ru(acac)(bpy)(dmso-*S*)(OH_2)](OTf) (**2**·(OTf))

A mixture of **P0** (0.44 g, 0.51 mmol) and Li(acac) (58 mg, 0.55 mmol) in acetone (100 mL) was stirred for 10 h at room temperature. The yellow solution gradually turned dark brown. The resulting dark-brown solution was evaporated to dryness under vacuum. The residue was dissolved in methanol (20 mL), and the solution was refluxed for 18 h. Heating for 1 h caused the yellow-brown solution to turn orange. The resulting orange solution was evaporated to dryness under vacuum and added with water (5 mL) to precipitate the orange complex *trans*-[Ru(acac)(bpy)(dmso-*S*)(OH_2)](OTf) (**2**·(OTf)). The precipitate was collected by filtration, washed with a small amount of cold water, and dried in vacuo (0.19 g, 60%). Orange crystals suitable for X-ray crystallography were obtained by concentrating an aqueous solution of **2**·(OTf) at 298 K. $C_{18}H_{23}F_3N_2O_7RuS_2$ (601.6): calcd. C 35.93, N 3.85, H 4.66; found C 35.79, N 4.59, H 3.82. ^{1}H NMR (300 MHz, D_2O): δ 9.28 (d, 2H, ^3J=5.6 Hz, H-6), 8.38 (d, 2H, ^3J=8.2 Hz, H-3), 8.10 (dd, 2H, ^3J=7.7 and 8.2 Hz, H-4), 7.67 (dd, 2H, ^3J=5.6 and 7.7 Hz, H-5), 5.52 (s, 1H, CH of acac$^-$), 2.79 (s, 6H, CH_3 of dmso), 2.16 (s, 6H, CH_3 of acac$^-$) ppm. Absorption spectroscopic data in water (nm, M^{-1} cm^{-1}): 284 (2.8×10^4) and 418 (4.4×10^3).

X-Ray Crystallography

For **1**·(OTf)·0.5H_2O, X-ray crystallography was performed at 173 K on a Rigaku Mercury 70 diffractometer with a CCDC detector using graphite-monochromated Mo-Kα radiation. For **2**·(OTf), X-ray patterns were obtained at 173 K on a Rigaku XtaLAB P200 diffractometer using multilayer mirror-monochromated Cu-Kα radiation. The structures were solved using direct methods [SIR92,[34] **1**·(OTf)·0.5H_2O; or SIR2011,[35] **2**·(OTf)] and refined using the full-matrix least-squares method with anisotropic thermal parameters for non-hydrogen atoms. The locations of hydrogen atoms were theoretically calculated using the riding model.

Supporting Information Summary

The Supporting Information contains details on the hydrogen bonding interaction in crystal of **1**·(OTf)·0.5H_2O, the ^{1}H NMR spectra of **1**·(OTf)·0.5H_2O in DMSO-d_6, acetone-d_6, and D_2O, the ^{1}H-^{1}H COSY of **1**·(OTf)·0.5H_2O in DMSO-d_6, the absorption spectra of **1**·(OTf)·0.5H_2O in DMSO and **2**·(OTf) in water, the isomerization of **1**·(OTf)·0.5H_2O to **2**·(OTf), the hydrogen bonding network of **2**·(OTf), and the ^{1}H NMR spectra of **2**·(OTf) in CD_3CN and D_2O. Deposition Numbers 2348269 (for **1**·(OTf)·0.5H_2O) and 2348270 (for **2**·(OTf)) contain the supplementary crystallographic data for this paper. These data are provided free of charge by the joint Cambridge Crystallographic Data Centre and Fachinformationszentrum Karlsruhe Access Structures service.

Acknowledgements

We would like to thank Prof. Noriharu Nagao (Meiji University, Japan) for his help in the X-ray crystallographic analysis of **1**·(OTf)·0.5H_2O. We also thank Editage (www.editage.jp) for English language editing.

Conflict of Interests

There are no conflicts of interest to declare.

Data Availability Statement

The data that support the findings of this study are available in the supplementary material of this article.

Keywords: Ruthenium(II) complex · Acetylacetonato anion · Ru(II)-dmso complex · X-ray crystallography · NMR spectroscopy · Isomerization · Hydrogen bonds

[1] O. Bysewski, M. Sittig, A. Winter, B. Dietzek-Ivanšić, U. S. Schubert, *Coord. Chem. Rev.* **2024**, *498*, 215441.
[2] V. Balzani, A. Credi, M. Venturi, *Coord. Chem. Rev.* **2009**, *38*, 1542–1550.
[3] A. Ito, D. J. Stewart, T. E. Knight, Z. Fang, M. K. Brennaman, T. J. Meyer, *J. Phys. Chem. B.* **2013**, *117*, 3428–3438.
[4] K. Hanson, D. L. Ashford, J. J. Concepcion, R. A. Binstead, S. Habibi, H. Luo, C. R. K. Glasson, J. L. Templeton, T. J. Meyer, *J. Am. Chem. Soc.* **2012**, *134*, 16975–16978.
[5] Y. Yamazaki, A. Umemoto, O. Ishitani, *Inorg. Chem.* **2016**, *55*, 11110–11124.
[6] V. Balzani, A. Juris, *Coord. Chem. Rev.* **2001**, *211*, 97–115.
[7] A. Vidal, D. Rossato, E. Iengo, G. Balducci, E. Alessio, *Chem. Eur. J.* **2023**, *29*, e202300893.
[8] S. Kumar, S. Singh, A. Kumar, K. S. R. Murthy, A. K. Singh, *Coord. Chem. Rev.* **2022**, *452*, 214272.
[9] C. Eidenschenk, L. Cheruzel, *J. Inorg. Biochem.* **2020**, *213*, 111254.
[10] M. G. Sauaia, E. Tfouni, R. H. de Almeiada Santos, M. T. do Prado Gambardella, M. P. F. M. Del Lama, L. F. Guimarães, R. Santana da Silva, *Inorg. Chem. Commun.* **2003**, *6*, 864–868.
[11] H. Jude, P. S. White, D. M. Dattelbaum, R. C. Rocha, *Acta Crystallogr.* **2008**, *E64*, m1388–m1389.
[12] B. Durham, S. R. Wilson, D. J. Hodgson, T. J. Meyer, *J. Am. Chem. Soc.* **1980**, *102*, 600–607.
[13] T. A. Word, A. Karolak, C. R. Cioce, A. Van Der Vaart, R. W. Larsen, *Comments Inorg. Chem.* **2016**, *36*, 343–354.
[14] Y. R. Pérez, L. D. Slep, R. Etchenique, *Inorg. Chem.* **2019**, *58*, 11606–11613.
[15] J. C. Dobson, T. J. Meyer, *Inorg. Chem.* **1988**, *27*, 3283–3291.
[16] B. J. Coe, T. J. Meyer, P. S. White, *Inorg. Chem.* **1993**, *32*, 4012–4020.
[17] B. J. Coe, C. I. McDonald, R. L. Beddoes, *Polyhedron.* **1998**, *17*, 1997–2007.

[18] D. Mishra, S. Naskar, R. J. Butcher, S. K. Chttopadhyay, *Inorg. Chim. Acta.* **2005**, *358*, 3115–3121.
[19] M. Toyama, D. Fujimoto, Y. Matsuoka, Y. Asano, N. Nagao, *Eur. J. Inorg. Chem.* **2018**, *2018*, 4349–4360.
[20] A. Vidal, R. Calligaro, G. Gasser, R. Alberto, G. Balducci, E. Alessio, *Inorg. Chem.* **2021**, *60*, 7180–7195.
[21] R. T. Ryan, D. Havrylyuk, K. C. Stevens, L. H. Moore, S. Parkin, J. S. Blackburn, D. K. Heidary, J. P. Selegue, E. C. Glazer, *Eur. J. Inorg. Chem.* **2021**, *2021*, 3611–3621.
[22] A. Dovletoglou, S. A. Adeyemi, T. J. Meyer, *Inorg. Chem.* **1996**, *35*, 4120–4127.
[23] L. Dudd, M. Hart, D. Ring, E. Sondaz, J. Bonvoisin, Y. Coppel, *Inorg. Chem. Commun.* **2003**, *6*, 1400–1405.
[24] S. Gupta, J. M. Vandevord, L. M. Loftus, N. Toupin, M. H. Al-Afyouni, T. N. Rohrabaugh, Jr., C. Turro, J. J. Kodanko, *Inorg. Chem.* **2021**, *60*, 18964–18974.
[25] S. J. Slattery, W. D. Bare, D. L. Jameson, K. A. Goldsby, *J. Chem. Soc. Dalton Trans.* **1999**, 1347–1352.
[26] R. Pettinari, F. Marchetti, C. Di Nicola, C. Pettinari, *Eur. J. Inorg. Chem.* **2018**, *2018*, 3521–3536.
[27] S. Li, G. Xu, Y. Zhu, J. Zhao, S. Gou, *Dalton Trans.* **2020**, *49*, 9454–9463.
[28] M. Allison, P. Caramés-Méndez, C. M. Pask, R. M. Phillips, R. M. Lord, P. C. McGowan, *Chem. Eur. J.* **2021**, *27*, 3737–3744.
[29] M. Toyama, K. Inoue, S. Iwamatsu, N. Nagao, *Bull. Chem. Soc. Jpn.* **2006**, *79*, 1525–1534.
[30] M. Toyama, S. Iwamatsu, K. Inoue, N. Nagao, *Bull. Chem. Soc. Jpn.* **2010**, *83*, 1518–1527.
[31] A. Gerli, J. Reedijk, M. T. Lakin, A. L. Spek, *Inorg. Chem.* **1995**, *34*, 1836–184.
[32] H. E. Gottlieb, V. Kotlya, A. Nudelman, *J. Org. Chem.* **1997**, *62*, 7512–7515.
[33] N. Nagao, M. Mukaida, S. Tachiyashiki, K. Mizumachi, *Bull. Chem. Soc. Jpn.* **1994**, *67*, 1802–1808.
[34] A. Altomare, G. Cascarano, C. Giacovazzo, A. Guagliardi, *J. Appl. Crystallogr.* **1993**, *26*, 343–350.
[35] M. C. Burla, R. Caliandro, M. Camalli, B. Carrozzini, G. L. Cascarano, C. Giacovazzo, M. Mallamo, A. Mazzone, G. Polidori, R. Spagna, *J. Appl. Crystallogr.* **2012**, *45*, 357–361.

Manuscript received: April 24, 2024
Revised manuscript received: August 12, 2024
Accepted manuscript online: August 19, 2024
Version of record online: October 17, 2024